

# Analysis of Wire Position and Operating Conditions on Functioning of NiTi Wires for Shape Memory Actuators

C. Zanotti, P. Giuliani, S. Arnaboldi, and A. Tuissi

(Submitted June 18, 2010; in revised form February 8, 2011)

In this work an experimental-numerical approach was used to analyze the thermo-mechanical behavior of thin NiTi wires, electrically heated, finalized to defining the influence of both wire position and the operating conditions of the actuator functioning. Tests were carried out on wires having diameters of 80 and 150  $\mu\text{m}$ , loaded by constant stresses of 100 and 200 MPa and characterized by DSC and strain/temperature hysteresis measurements. Two wire positions (horizontal and vertical) were adopted in single cycle tests and designed to obtain different typologies of the heating and cooling transients. In general, the heating time was selected to reach a steady state condition while the cooling time always allowed decreasing the wire temperature to the ambient one. Data concerning strain, applied current and voltage were simultaneously acquired during the tests. Moreover, for the optimization and validation of a numerical model, for the 150  $\mu\text{m}$  wire in diameter was used, its temperature was recorded by IR thermographic system. On the basis of the collected experimental data, a simple model was tested to reproduce the experimental results and data regarding the heat exchange coefficient and wire electrical resistivity dependence on temperature were obtained. The influence of the experimental wire positioning and wire diameter on the free convection coefficient is reported and the results indicate that the heating transient is associated with different convection coefficients depending on the heating modalities.

**Keywords** martensitic transformation, NiTi shape memory alloys, shape memory actuators, SMA modeling

## 1. Introduction

Shape memory alloys (SMAs) exhibit unusual thermo-mechanical characteristics such as the shape memory effect (SME) and the superelasticity (SE). These unique properties are due to a reversible martensitic transformation, occurring at the solid state, between two phases, the so-called *austenite* and *martensite* (Ref 1). SME takes place when the material is strained at low temperature, in its martensitic state, deformation values of the order of 6-8% can be restored by heating the material above the transformation temperatures range. On the other hand, if the material is loaded, in its high-temperature austenite phase, deformation of the order of 10-12% can be completely recovered on unloading; this is called SE behavior. From practical point of view, SE makes it possible to manufacture of several commercial SMA devices, mainly for the biomedical field while, the SME is used for the development of smart actuators, fasteners and couplings, gadgets,

This article is an invited paper selected from presentations at Shape Memory and Superelastic Technologies 2010, held May 16-20, 2010, in Pacific Grove, California, and has been expanded from the original presentation.

C. Zanotti and P. Giuliani, Institute for Energetics and Interphases, Via R. Cozzi 53, Milan, Italy; and S. Arnaboldi and A. Tuissi, Institute for Energetics and Interphases, Corso Promessi Sposi 29, Lecco, Italy. Contact e-mail: tuissi@ieni.cnr.it.

### List of symbols

$A_1$	Lateral area of the wire
$A$	Wire cross-section area
$c_0$	Specific heat
$h$	Free convection coefficient
$c_M$	Specific heat (martensite)
$I$	Current
$K_a$	Air thermal conductivity
$\Delta H$	Latent heat of transformation
$L_i$	Wire initial length
$L$	Wire length
$m$	Wire mass
$Nu$	Nusselt number
$P_{el}$	Electrical power
$P_m$	Mechanical power
$t$	Time
$d$	Wire diameter
$L_c$	Characteristic length
$T$	Wire temperature
$T_a$	Ambient temperature
$V$	Voltage
$c_A$	Specific heat (austenite)
$v$	Deformation velocity
$V_w$	Wire volume
$W$	Weight
$\sigma$	Wire stress
$\varepsilon_T$	Wire total emissivity
$\rho$	Wire resistivity
$\varepsilon$	Wire strain
$\varepsilon_{max}$	Maximum wire strain
$\xi$	Austenite volume fraction
$\sigma_B$	Stefan-Boltzman constant
$L_d$	Force

hybrid composites (Ref 2-4). Among several SMAs, the Ti-rich NiTi system shows the largest recoverable strain values (up to 8%) joint to a good workability and represents the principal compound for the development of shape memory devices. Thus, world-wide engineering efforts are oriented toward the manufacturing of NiTi semifinished products in the form of rods, plate, wire, tape, ribbon, thin film with tailored and repeatable characteristics as active SMA elements. It is demonstrated that NiTi wire can be processed and trained to obtain large recoverable strain values (4%), also under an applied force, with excellent cycling stability (over 100,000 thermo-mechanical cycles) (Ref 5), and it seems to be the most suitable product for the manufacturing of the shape memory electromechanical actuators. It was also demonstrated that SM devices are specifically efficient, at low dimensions, because of their high power/weight ratio with respect to the other actuating technologies (Ref 6) and in the recent years commercially available thin NiTi wires, down to 15-20  $\mu\text{m}$  in diameter as well as thin films and plates, are favouring the development of promising mini and micro SM actuators (Ref 7-9).

It is well-known that the functional properties of SM actuators depend on the thermo-mechanical manufacturing history of the SMA elements; however, significant property adjustment, as well as device energy efficiency, can be reached through a deeper knowledge of the phenomena governing the actuator heating and cooling transients. Furthermore, it is experimentally demonstrated that transformation temperatures can be significantly modified by changing the external force, according to the linear Clausius-Clapeyron relationship (Ref 10), but it is not clear what the role these temperature changes may be on the frequency response of the actuator. Of course, it is easy to speed up the wire heating by increasing the electrical power (Joule's effect), while the wire cooling rate, mainly driven by free convection phenomena, can be increased by modifying the wire configuration (vertical or horizontal) and/or adopting an active cooling process; on the latter aspects there are very few experimental data available. The possibility to simulate the response time of SMA wires can make the actuator design easier. Thus, the analysis of SME dynamic phenomena becomes interesting for actuator applications. The capability of performing accurate simulations of the heating and cooling transient of electrically heated wires depends strongly on the correct definition of the thermo-mechanical properties of NiTi SMA wires and on the determination of the influence of the operating conditions.

The mechanical response of loaded thin NiTi wires is generally analyzed with pseudoelastic models describing the thermo-mechanics of the wire. Several numerical approaches were proposed including scientifically rigorous and realistic models useful for SM actuators design. Among these the recent paper (Ref 11) reports a complete review of the modeling methods regarding single crystals dealing with the phase transformation and presents the basic properties of SMAs while aspects dealing with the micromechanical modeling of polycrystalline SMAs are discussed in Ref 12. However, to simplify the numerical approach, thermo-mechanical models for SMA wires, under uniaxial loading, were also proposed. In fact, Bhattacharyya (Ref 13) presented a comparison between the experimental results and simulations computed adopting a phenomenological model considering the Nusselt number dependence on surrounding air properties through the Rayleigh and Grashof numbers. The main indication emerging from this work regards the convection coefficient that increases with the

electrical current is, for heating, significantly higher than for cooling. Moreover, Bhattacharyya (Ref 13) did not provide any information on the influence of the wire diameter and position on the convective coefficient. Following this approach, other papers are reported in literature (Ref 14-18) but, in all these cases, the convective coefficient value used in the numerical computations was independent of temperature.

The main scope of this article is to analyze the heating/cooling behavior of thin NiTi wires under several working conditions (heating current, applied force, wire position, and wire diameter) throughout an experimental-numerical approach to define the heat exchange coefficient by the evaluation of the Nusselt number for the horizontal and vertical configuration.

As the phase transformation in NiTi wires is driven by the temperature and stress fields it is necessary to verify the influence of the A-M transformation on the cooling time to be able to define the operating frequencies of the actuators.

Finally, the experimental procedure allows estimating the wire resistivity during the heating and cooling transients, wire temperature and strain indicating the influence of the phase transformation on these parameters.

## 2. Experimental Methodology

Particular care was put in material preparation where a Ni49Ti51 (at.%) alloy was vacuum induction melted and then hot and cold processed to wire. Cold drawn wires, of 150 and 80  $\mu\text{m}$  in diameter, were strand annealed at 430  $^{\circ}\text{C}$ , for 10 min. After water quenching all the batches were subjected to 500 thermo-mechanical cycles, under constant stress of 250 MPa, to stabilize the functional properties. Differential scanning calorimetric scans were carried out by a TA Instruments<sup>®</sup> (DSC Q100) and strain-temperature hysteresis measurements of 80  $\mu\text{m}$  trained wires, under a constant stress 200 MPa, were performed in a DMA (TA Instruments DMA Q800) and these results were used for numerical model validation.

The experimental work was aimed at obtaining the operating parameters that guarantee the fastest wire cooling when free convection is the unique phenomenon driving the heat exchange. For this reason, two self-assembly systems were designed and a schematic view of the experimental apparatus used to analyze the heating/cooling transients of the vertically positioned wire is reported in Fig. 1. That depicts the wire hanging from a frame where the constant stresses were applied by the axial weights fixed to the lower end of the wire. This vertical test configuration has been adopted for long time for thermo-mechanical testing of electrically heated wires under constant stresses (Ref 19). Once this apparatus is rotated by 90 $^{\circ}$  the tests can be carried out horizontally: picture of this experimental configuration is shown in Fig. 2 where the wire is attached to the force by using a pulley equipped with a low-friction bearing. In both cases, to avoid constraints, due to the electrical wire connections, able to generate anomalous stress or lateral movements during the wire shortening, a mercury bath was used as free electrical contact.

An electrical circuit was connected to the two SMA wire leads (100 mm in distance) and a current source, supplying heating and cooling currents, was controlled by a PC. Wire deformation during each thermo-mechanical cycle, was detected by a laser optical proximity sensor (resolution 20  $\mu\text{m}$ ). Wire temperature was measured only in the case of

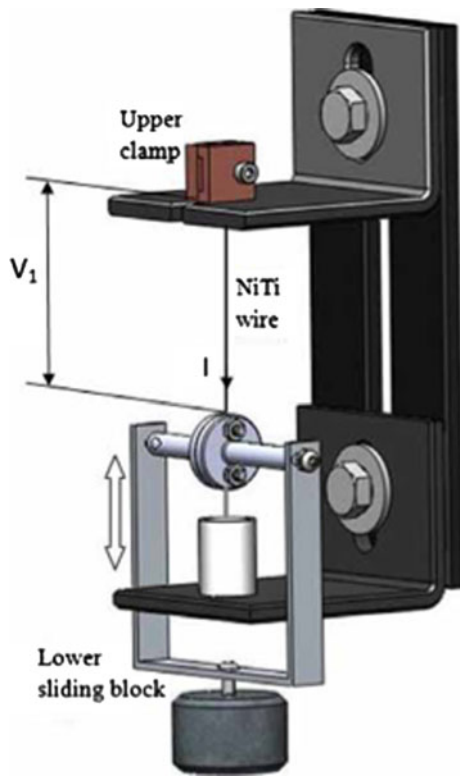


Fig. 1 Sketch of the experimental vertical configuration

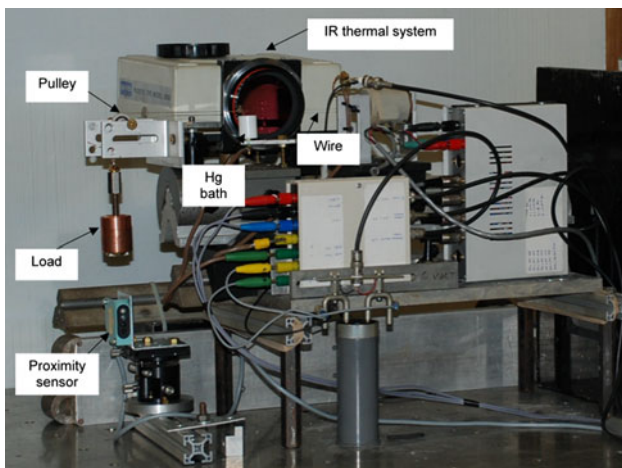


Fig. 2 Picture of the experimental horizontal configuration

the 150  $\mu\text{m}$  wire because of the limited spatial resolution of the IR apparatus (thermal video system Hughes series 3000), The constant sampling frequency was 50 Hz. Applied current ( $I$ ), voltage ( $V$ ), and wire deformation were then acquired simultaneously using a sampling frequency that guarantees to store during a single cycle, at least,  $10^5$  data for each parameter.

The experiments were aimed at defining the effect of the current, force, and wire diameter on the wire deformation behavior while, in order to elaborate on the influence of the heating and cooling dynamics, the wire was tested using two different modalities (dynamic vs. quasi-steady). In the case of the dynamic modality, a square wave current is generated while in the case of quasi-steady condition a trapezoidal current form, characterized by long heating and cooling times, was chosen.

### 3. Numerical Approach

1-D models (Ref 14, 16, 17) have been used to investigate the deformation mechanism based on detailed descriptions of the transformation rate and generally, results indicate that the overall temperature response and thus the displacement response is mainly driven by the heat convection phenomenon. For this reason, this approach considers a simple empirical model that does not incorporate physical aspects describing the nature of phase transformation but it can be useful for obtaining practical information concerning the influence of the operating conditions on the SMAs wire response time. Nevertheless, this approach, based on the integration of differential equation, gives accurate simulations of the experimental results (Ref 13) once the convection coefficient dependence on temperature is defined.

The condition of using the 0-D model supposes that the heat conduction in the wire and the clamps can be neglected and a similar approach was also considered by Meier (Ref 15) proposing a 0-D numerical approach to wire thermo-mechanical modeling.

Computations are based on the following assumptions: electrical power is the only external heating source, wire volumetric heating is supposed, the temperature distribution in the sample is uniform, wire heat capacity depends on temperature and transformation rate, heat losses by free convection are defined by the heat exchange coefficient temperature dependence while those concerning radiant emission are accounted for by a constant value of the total wire emissivity. The contribution of the mechanical work done by the wire during its deformation is considered too.

The numerical code integrates, by using the fourth order Runge-Kutta method, the following ordinary differential equation:

$$P_{el} = mc_0 \frac{dT}{dt} + m\Delta H \frac{d\xi}{dt} + L_d \frac{d\varepsilon}{dt} + hA_1(T - T_a) + \sigma_B \varepsilon_T A_1 (T^4 - T_a^4) \quad (\text{Eq 1})$$

and the initial boundary condition is:  $T(t = 0) = T_a$ .

In particular, the left-side term of Eq 1 represents the electrical power absorbed by the wire while the other terms, on the right side, define, respectively: the thermal power stored in the wire, the thermal power related to the M-A transformation, mechanical power necessary to pull up the force, the thermal power lost by free convection and radiation. Of course, some terms of Eq 1 must be properly defined to indicate their contribution during the heating or the cooling transients.

Besides the wire contraction, in consequence of the SME, an opposite thermal expansion should be accounted for (Ref 15, 18). Considering that thermal strain is two order of magnitude lower than the one associated to the phase change, in this work this consideration it was not taken into account and  $\xi$  was evaluated by the experimental values of  $\varepsilon$ . Thus, the austenite volume fraction was approximated as:  $\xi = \varepsilon/\varepsilon_{\text{max}}$ .

Many more parameters of Eq 1 were defined by the experimental results (current, voltage, and strain) such as  $P_{el} = VI$ ,  $L = L_i + \varepsilon$ ,  $A = V_w/L$ ,  $A_1 = \pi dL$ ,  $\rho = (VA)/(IL)$ .

The specific heat temperature dependence has been taken from data reported by Smith (Ref 19) while the following expression has been used in the transformation temperature range  $c_0 = c_M(1 - \xi) + c_A\xi$ . The values of the parameters necessary to integrate the Eq 1 are reported in Table 1 while all

**Table 1 Parameters used for numerical computation**

$C_M$	470	J/kg · K	Ref 3
$C_A$	480	J/kg · K	Ref 3
$\Delta H$ (heating)	22,000	J/kg	Authors
$\Delta H$ (cooling)	18,000	J/kg	Authors
$\varepsilon_T$	0.3	...	Ref 25

the other terms are estimated from the experimental results. Dependence of the free convection coefficient on the gas properties and operating conditions is defined by the common expression:  $h = NuK_a/L_c$ .

$Nu$  is defined considering the wire position and its dependence on Rayleigh and Prandtl numbers (Ref 20, 21) and generally its value is larger when the wire is positioned vertically. However, it must be considered that in the case of the vertical wire position  $L_c = L$ , while for the horizontal case  $L_c = d$  so, the  $h$  value must be independent of  $d$  when placed vertically and independent of  $L_c$  when positioned horizontally.

Of course, to validate this simple model the wire temperature history must be measured or indirectly estimated and so two different approaches have been followed depending on the wire diameter. When  $d = 150 \mu\text{m}$  the wire temperature is directly measured, instead in the case of  $d = 80 \mu\text{m}$  a correlation between one of the measured parameter and the temperature is required. Here, results of strain/temperature hysteresis tests have been used to constrain the numerical solution.

## 4. Experimental Results

As previously reported, wire deformation, applied current ( $I$ ), and voltage ( $V$ ) were acquired during the tests, while, in the case of  $150 \mu\text{m}$  wire, also the temperature was recorded by a thermal video system (IR). As thin wire applications are more promising, and also for matter of space, the presented results mainly concern the experiments obtained testing the  $80 \mu\text{m}$  wires.

To define the influence of electrical current, force, and wire position on the wire heating and cooling transients, tests carried out adopting the dynamic modality (wire heated by a 10 s current pulse) are analyzed first. In this case, the cooling rate only depends on the heat transfer coefficient once the experiments are performed using the same operating conditions. The features of the results obtained performing this kind of tests are similar: generally wire deformation during the heating transient occurs in  $<1$  s while, the wire cooling transient, driven only by the heat loss phenomena by radiation and free convection, takes about 4 s to final recovery of the initial length. By the knowledge of the applied current, voltage, and deformation, electrical resistivity and strain rate dependence on time can be evaluated.

Several tests regarding the  $80 \mu\text{m}$  wire, horizontally positioned (length = 100 mm and electrical resistivity =  $88 \times 10^{-6} \Omega \cdot \text{cm}$ ) were performed and the typical results obtained driving the wire heating by a 200 mA current and loaded by a stress of 200 MPa are depicted in Fig. 3.

In this case, the wire deformation reaches its maximum value of 3.9 mm and it stays constant until the current drops to zero. The voltage ( $V$ ) shows a different trend: in fact, at the beginning, the voltage starts from the initial value of 3.65 V

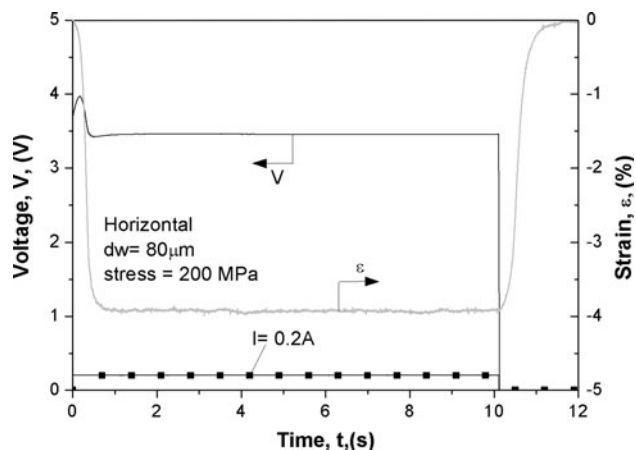


**Fig. 3** Experimental acquired data for a test driven by a square wave current

and then it increases up to a maximum value of 3.97 V, then it decreases till it reaches its minimum value (3.42 V). The  $V$  behavior is associated to the geometrical changes due to the shrinking of the wire as well as the high resistivity of the intermediate R-phase during the M-R-A transformation. Once the transformation is completed, its value is constant (3.45 V) but lower than the one measured at the beginning of the test. In order to define the influence of the operating conditions on the wire behavior a detailed analysis of the initial and final parts of the transient was carried out comparing the wire deformation and deformation rate.

The main effect of the current increase is to increase the electrical power absorbed by the wire and, which also entails a wire temperature surge. Results of the effect of the heating currents with pulses of 10 s, for the  $150 \mu\text{m}$  wire, on the max/min wire temperature and the recovered strain are reported in Table 1. For the  $80 \mu\text{m}$  wires, the influence of the heating current was evaluated by comparing two cycles (wire horizontally placed) driven by two current values (200 and 240 mA): the heating/cooling transients are reported in Fig. 4(a) and (b), respectively. In Fig. 4(a), it is evident that the larger current has the effect of speeding the heating process (higher deformation rate) and to promote a larger deformation value, because a higher wire temperature is reached (see Table 2). The cooling transient (Fig. 4b) indicates that deformation time is longer for the larger current and this occurrence appears to be dependent on the larger thermal energy left stored in the wire when the current is switched off ( $T_{\text{max}}$  is higher and  $C_p$  is larger too). The effect of the force has been investigated by comparing two tests (wire horizontally placed, current 200 mA) carried out using different stress values (100 and 200 MPa) and the results are reported in Fig. 5(a) and (b). In this case it needs to be considered that the transformation temperatures are affected by the applied force, as predicted by the Clausius-Clapeyron relationship. The heating transient (Fig. 5a) indicates that a larger stress induces larger deformation but lower deformation rate; the latter could be only associated with wire stress and dynamics. An opposite trend is found considering the cooling transient (Fig. 5b) that is mainly driven by the force applied to the wire. In fact, a larger stress (200 MPa) induces higher transformation temperature, higher deformation rate and faster recovering of the initial length because, in this case, the force is the only active force driving the wire elongation.

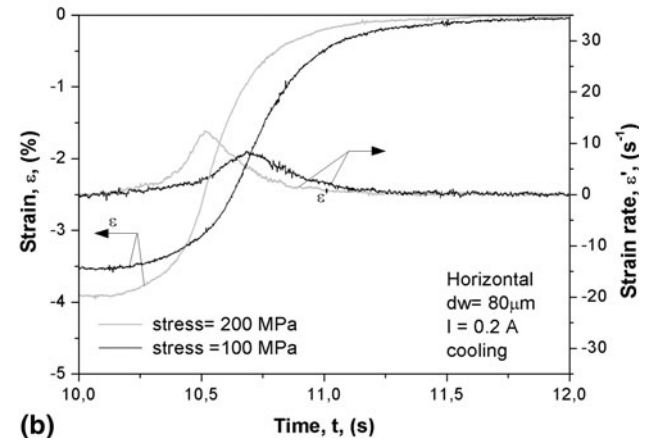
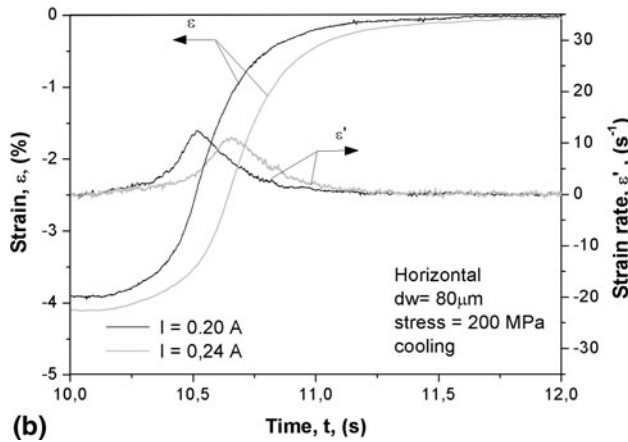
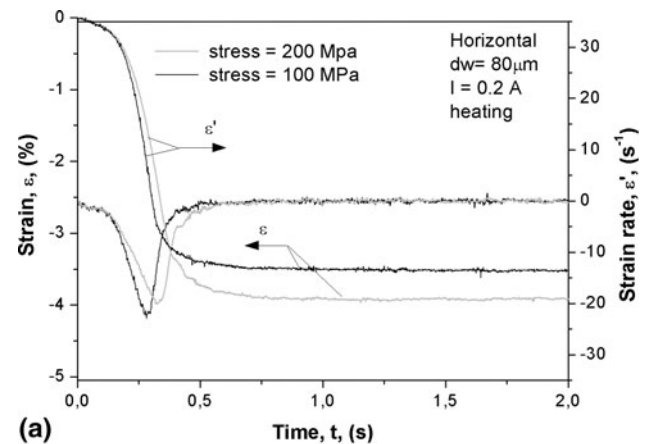
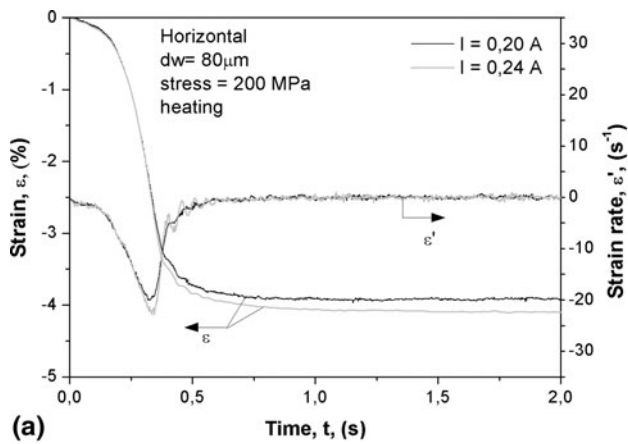


Fig. 4 (a) Influence of the driving current on the heating transient and (b) influence of the driving current on the cooling transient

Fig. 5 (a) Influence of the applied load on the heating transient and (b) influence of the applied load on the cooling transient

**Table 2** Dependence of wire temperature  $T$  and recovered deformation,  $\epsilon$  on electrical current (stress 200 MPa, square wave)

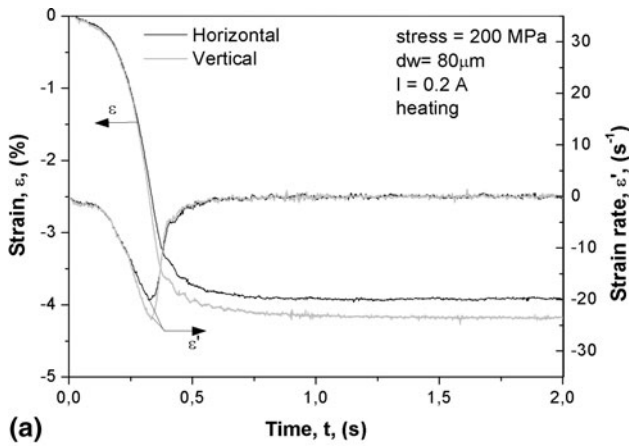
Current, mA	$T_{max}$ , K	$\epsilon$ , %
300	348	2.96
350	390	4.4
400	408	4.54
450	442	4.62
500	457	4.67

The effect of the wire position (vertical and horizontal) has been defined comparing tests performed using the same operating conditions (200 mA, 200 MPa, current pulse 10 s). Curves describing the heating transient, reported in Fig. 6(a), show that the vertical configuration promotes larger deformation in a shorter time. That indicates that temperature increases faster reaching higher values and it means that the  $h$  value is lower in this configuration. The cooling transient (Fig. 6b) can be explained by the same phenomenon (lower  $h$  value): as the deformation rate is lower in the case of the vertical configuration, the wire recovers the initial length in longer time.

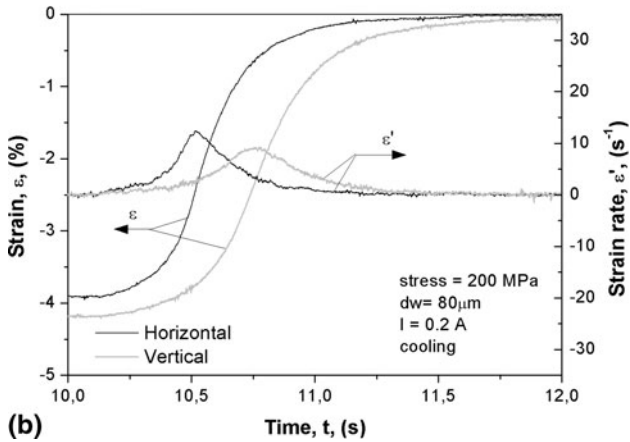
This analysis indicates that the heat exchange coefficient plays an important role because it can influence the maximum deformation and wire temperature as well as the deformation rate. Moreover, these tests allow comparing the values of the

electrical resistivity, only associated with the wire heating process, that can be calculated knowing of the voltage ( $V$ ), applied current ( $I$ ), wire length ( $L_w$ ), and wire diameter ( $d_w$ ). The results of this comparison are reported in Fig. 7. Thus, four curves are presented and it is evident that their shapes are similar to the voltage one (see Fig. 3). It can be noticed that the highest resistivity values correspond to curves 1 and 2 (highest wire temperatures) which are mutually similar. Conversely, curve 3 differs from curve 4 (both measured for 0.2 A) because a shift toward lower values of resistivity is produced when stress is decreased. In this case, the stress is the main parameter that influences the electrical resistivity. In fact, the resistivity of this wire at 295 K (room temperature) is  $88.6 \times 10^{-6} \Omega \cdot \text{cm}$  when unloaded,  $91 \times 10^{-6} \Omega \cdot \text{cm}$  when the force is 100 MPa and  $93 \times 10^{-6} \Omega \cdot \text{cm}$  for 200 MPa ( $t = 0$  s); that could be related to a different degree of detwinning of the martensite domains as a function of the applied force. As expected, resistivity values, after the heating transient when the deformation is constant, is, for all the tests, higher than the corresponding values at the beginning ( $T = 295$  K): that is due to the high-austenite phase resistivity. Further remarks and details on the resistivity of NiTi wires are reported in the Appendix.

The same wire has been tested adopting the quasi-steady modality (trapezoidal current) to confirm the results obtained under dynamic conditions and to add more details concerning the wire cooling transients. In fact, this modality allows measuring the voltage during the wire heating and cooling and



(a)



(b)

Fig. 6 (a) Influence of the wire position on the heating transient and (b) influence of the wire position on the cooling transient

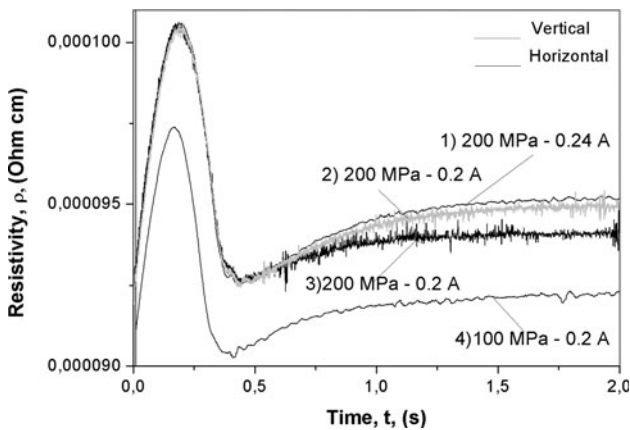
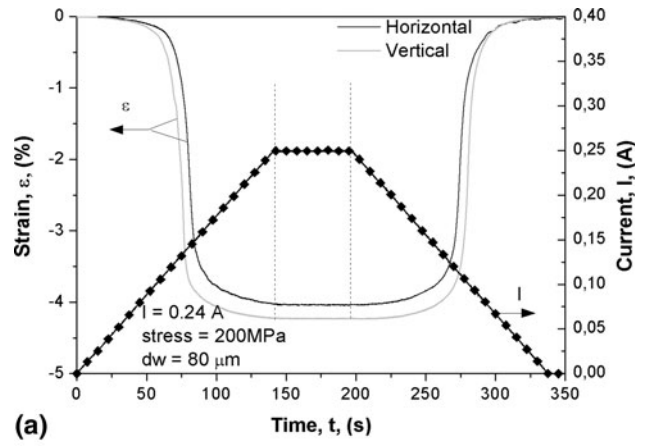
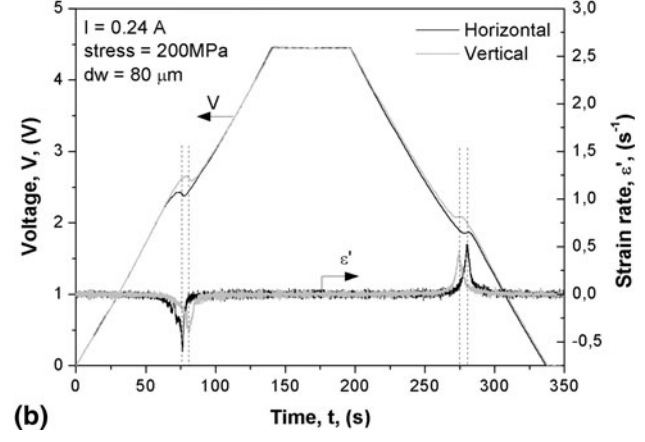


Fig. 7 Comparison of the evaluated resistivity for different tests

thus makes it possible to calculate the resistivity for both cases. Figure 8(a) and (b) report the comparison of variables between vertical and horizontal position, while Fig. 9(a) and (b) report the influence of the applied stress. These results indicate clearly the effect of the different operating conditions on the voltages applied to the wire and more interesting by the presence, during the cooling transient, of the A-M transformation. All the results indicate and confirm the general observations made for the tests adopting the dynamic modality.



(a)



(b)

Fig. 8 (a) Trapezoidal current (deformation and current) wire position effect and (b) trapezoidal current (voltage and deformation rate) wire position effect

## 5. Numerical Results

Numerical simulations are mainly aimed at defining the temperature dependence of the heat exchange coefficient, electrical resistivity, and occurrence of the hysteresis phenomena. In order to meet this aim, the wire temperature must be known and for this reason simulations have been carried out using data derived from the testing of a 150 μm wire.

In the following in order to give a picture of the applied methodology, the case is reported where the current is a trapezoidal waveform with the same rate of current both in the increasing and decreasing steps (12.5 mA/s). The simulation proposes to reproduce the test carried out in the horizontal configuration with the applied current, voltage, deformation, and wire temperature dependence on time reported in Fig. 10. Here, the comparison between the computed and experimental wire temperature histories is presented too and the overlapping of the data has been obtained by defining appropriate heat exchange coefficient  $h(T)$ . These data indicate that voltage and temperature start to get lower when current decreases while deformation begins its drop later on suggesting that the hysteresis phenomena occur during the wire cooling. Moreover, the graph clearly shows the effect of the M-A-M transformations on the voltage ( $V$ ) and wire temperature and these peculiarities can be associated with the electrical resistivity changes. In fact, as shown in Fig. 11, the deformation rate curve presents two peaks and the electrical resistivity curve

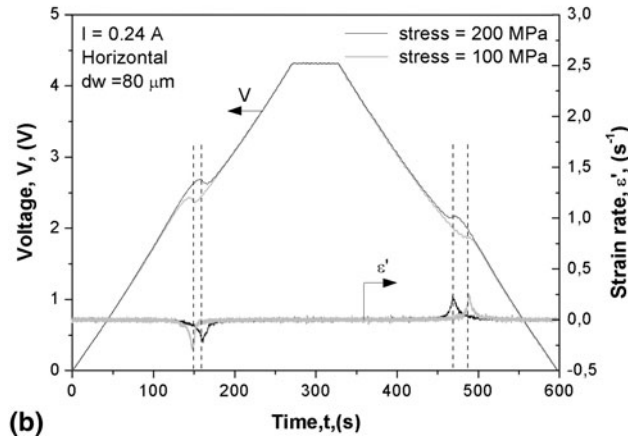
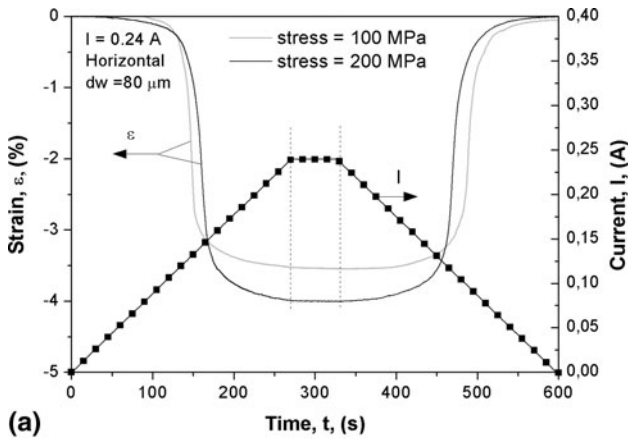


Fig. 9 (a) Trapezoidal current (deformation and current) stress effect and (b) trapezoidal current (voltage and deformation rate) stress effect

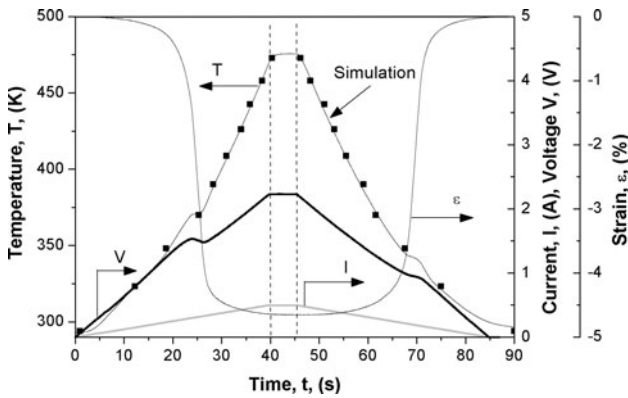


Fig. 10 Experimental results 150 μm wire

indicates a resistivity decreasing across the positive peak while the opposite behavior is shown across the negative peak. The two peaks can be associated with the maximum M-A transformation rate during the wire heating (positive value) and maximum A-M transformation rate during the wire cooling (negative value).

Once the calculated temperature history fits the experimental result (Fig. 10), other information, regarding the influence of the contribution of the terms reported in Eq 1 on the wire energy balance, are also and are depicted in Fig. 12. Here, a

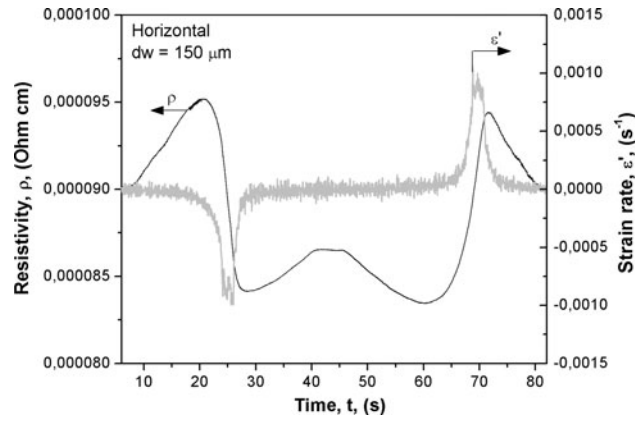


Fig. 11 Evaluated results of the 150 μm wire

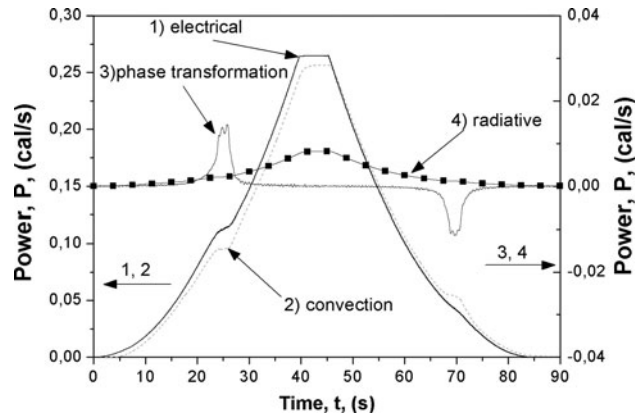


Fig. 12 Comparison between experimental and numerical results (150 μm wire)

comparison between the applied electrical power (curve 1) and powers (curves 2, 3, and 4) dissipated by the wire allows a full description of what are the most important processes affecting the heating and cooling transients. It is evident that under this experimental configuration the power lost by free convection is the main term governing the response of the wire and that the wire heating requires only a few percent of the absorbed electrical power.

Moreover, the numerical evaluation of the wire temperature history allows an analysis of the dependence of other parameters on temperature. The most interesting one are reported in Fig. 13, where the electrical resistivity and wire deformation indicate the occurrence of the hysteresis phenomena that induce a shift in temperature of about 30 K.

Numerical simulations of tests, carried out by using wires horizontally positioned and heated by a trapezoidal current time dependence, are computed integrating Eq 1 and results are depicted in Fig. 14. Data regarding the 80 μm wire were obtained without any knowledge of the wire temperature, because no experimental data were available, but trying to reproduce experimental information obtained by thermo-mechanical and calorimetric experimental measurements (hysteresis curve).

These curves (heating and cooling) indicate that, if the wire heating and cooling transients are driven by same current profile,  $h$  is almost the same. The values are, however, different

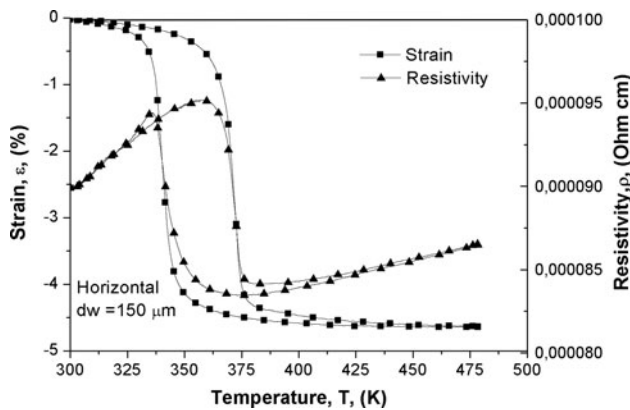


Fig. 13 Estimated wire deformation and electrical resistivity (150  $\mu\text{m}$  wire)

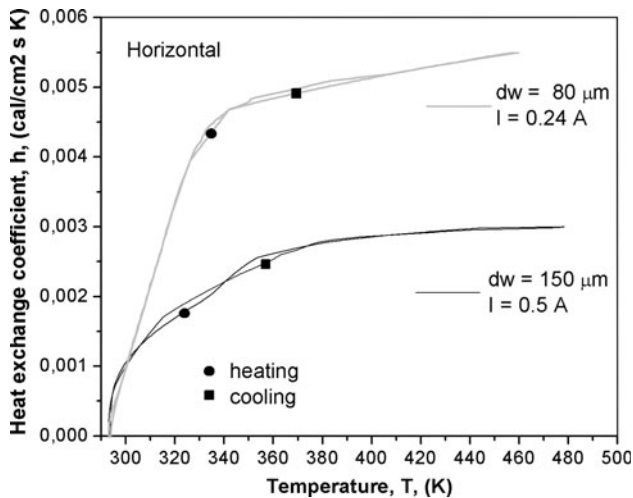


Fig. 14 Comparison between heat exchange 150 vs. 80  $\mu\text{m}$  wires

for different wire diameters in fact, if the ratio:  $hr = h[80 \mu\text{m}]/h[150 \mu\text{m}]$  is estimated the following relation can be written  $1.8 < hr < 2$  indicating that  $h[80 \mu\text{m}]$  is about 90-100% larger than  $h[150 \mu\text{m}]$ .

As in the definition of  $h$ , the wire diameter represents the characteristic length,  $hr$  is associated with the wire diameter ratio  $d[150 \mu\text{m}]/d[80 \mu\text{m}]$  that, in this case, is 1.87. This result confirms that the wire size is the most important parameter defining the heat exchange coefficient and comparisons between results regarding the wire position show that the  $h$  for the horizontal configuration is about 22% larger than the value for the vertical one.

A last remark can be made about the influence of the dynamic experimental procedure (square wave) on the heating transient and the most important changes of the heat exchange coefficient. As previously mentioned, the power lost by free convection is the main term governing the response of the wire and also in this case the wire heating requires only few percent of the absorbed electrical power once the maximum temperature is reached. In general, the wire cooling, driven only by free convection, is characterized almost by the same temperature dependence of the  $h$  coefficient, while different values had to be used for describing the heating transient. This fact has been highlighted by simulating the results of tests characterized

by a electrical current of 0.5 A and a pulse duration of 8 s that can be compared with the results presented for in Fig. 10-12. The main observation regards the larger values of maximum temperature and strain measured in the case of the current pulse indicating that this modality exploits better the applied electrical power and this statement is supported by the comparison between the absorbed electrical energy and the one released by free convection during the transient to reach the maximum wire temperature. In fact, when pulse current has been used the free convection energy is about 77.5% of the electrical one while, in the case of trapezoidal current, it is about 92%. It goes without saying that, speeding the wire heating tends to reduce the effect of the convection process because the latter is not an instantaneous phenomenon and this aspect has been indicated in Ref 22 that presents, in Fig. 10, the asymptotic trend of wire heating time.

Finally, it is important to stress that the  $h$  coefficient, during the wire heating presents a peak in correspondence of the larger deformation rate because, under this condition, the  $Nu$  number increases during the wire deformation. Moreover, the peak value can be twice as large as the  $h$  coefficient estimated at the maximum wire temperature. Differences between the  $h$  coefficient for heating and cooling were indicated by Bhattacharyya (Ref 13) that also found the effect of the dynamics on this parameter. In fact, he reported that the  $h$  value, estimated by testing a wire having a diameter of 360  $\mu\text{m}$  and heated by a current ranging between 0.9 and 1.3 A, increases with the electrical current augmentation demonstrating that a faster deformation tends to improve the  $Nu$  number. Considering that the wire diameter used in Ref 13 was four times bigger than the one tested (80  $\mu\text{m}$ ) in this work we can expect, on the basis of the result presented in Fig. 14, an  $h$  value of about 0.0013  $\text{cal}/\text{cm}^2 \text{ s K}$ . The results of  $h$ , reported in Fig. 9 of (Ref 13), are in good agreement with this simple calculation as they range between 0.0012 and 0.0014  $\text{cal}/\text{cm}^2 \text{ s K}$ .

## 6. Conclusions

Wires with diameters of 80 and 150  $\mu\text{m}$  have been experimentally tested under constant stresses of 100 and 200 MPa adopting two wire positions (horizontal and vertical), in order to define the effect of the convection phenomena on the wire heating and cooling transients. Tests were conducted forcing the wire deformation by single current pulses adjusted to obtain different deformation rates and simultaneously acquiring current, voltage, strain, and wire temperature. In order to generate different temperature fields around the wire heating history can be tailored choosing the suitable current dependence on time. Starting from these data, numerical simulations were computed based on a simple 0-D model aimed at reproducing the experimental temperature history and/or the hysteresis curve. The influence of the wire diameter, wire position, and deformation rate on the heat exchange coefficient have been described. Results demonstrate that the wire diameter is the main parameter that can strongly modify the heat exchange coefficient (about 100% increasing when  $d_w$  decreases from 150 to 80  $\mu\text{m}$ ) while wire position, although comparatively less important, still produce a significant augmentation (about 22% moving from vertical to horizontal configuration) of the same coefficient. Moreover, results regarding the effect of the operating conditions indicate that

wire temperature and stress are the most important parameters affecting the value of the electrical resistivity.

## Appendix

Electrical resistivity ( $\rho$ ) has been evaluated with knowledge of wire length ( $L$ ), applied current ( $I$ ), and voltage ( $V$ ) at the wire ends. Both  $L$  and  $V$  are dependent on (i) wire temperature and (ii) M-A transformation that occurs within a defined temperature range.

In general, the temperature distribution along the SMA wire, because of possible macroscopic difference in the Austenite/Martensite ratio, localized deformations, and heat losses at different positions, is spatially nonuniform. Thus, the evaluated  $\rho$  values of this work represent an average wire resistivity. However, when horizontal configuration and slow heating/cooling transients were adopted, the wire temperature can be well approximated by the uniform distribution. In fact, long heating times decrease the temperature difference between the wire ends and the clamps, so the heat transferred from the wire to the clamps is limited. Moreover, these operating conditions allow minimize the heat losses close to the clamps because the heat exchange coefficient ( $h$ ) decreases due to the different geometry that affects the “characteristic length” parameter for evaluating Nusselt’s number. This occurrence does not reduce significantly the temperature of the wire close to the clamps and this aspect was observed when the wire temperature was measured using the IR apparatus.

More critical is the wire temperature nonuniformity when the vertical configuration was adopted. In this case, the  $h$  value changes along the wire length and near the upper clamp the fluid velocity tends to zero generating a localized stagnation point. As a consequence, near the upper clamp the Nusselt number is less than the one along the wire and the temperature reaches its maximum value. For these considerations, the electrical resistivity evaluation, supposing that the wire temperature is uniform, is not far from the real case when horizontal configuration was chosen and the 0-D model can be used especially for simulating experiments carried out under quasi-steady conditions.

The results presented show a resistivity decrease of about 12% when the strain varies from 0.4% (martensite) to 4.4% (austenite). This value is in good agreement with  $\rho$  variation of 13% reported in the Ref 23. Again, detailed results on the influence of the force on the resistivity has been recently reported in Ref 24, where the authors show the  $\rho$  increase with force raise, the shift of the resistivity peak toward higher temperatures and the dependence of resistivity on the investigated phases (austenite, R, and martensite). The reported conclusions are in good agreement with the results obtained in this work.

## References

1. K. Otsuka and C. Wayman, Mechanism of Shape Memory Effect and Superelasticity, *Shape Memory Materials*, K. Otsuka and C. Wayman, Ed., Cambridge University Press, Cambridge, 1998, p 27–48
2. J. Van Humbeeck, Non Medical Applications of Shape Memory Alloys, *Mater. Sci. Eng. A*, 1999, **273–275**, p 134–148
3. T. Duerig, A. Pelton, and D. Stockel, An Overview of Nitinol Medical Applications, *Mater. Sci. Eng. A*, 1999, **273–275**, p 149
4. Y. Yeager, A Practical Shape Memory Electromechanical Actuator, *Mech. Eng.*, 1984, **106**, p 52–55
5. A. Tuissi, P. Bassani, A. Mangioni, L. Toia, and F. Butera, Fabrication Process and Characterization of NiTi Wires for Actuators, *Proceedings of SMST 2004*, M. Mertmann, Ed., 2006, p 501–508
6. K. Ikuta, Micro/Miniature Shape Memory Alloy Actuator, *Proceedings 1990 IEEE International Conference on Robotics and Automation*, 1990, p 2156–2161
7. A. Nespoli, S. Besseghini, S. Pittaccio, E. Villa, and S. Viscuso, The High Potential of Shape Memory Alloys in Developing Miniature Mechanical Devices: A Review on Shape Memory Alloy Mini-Actuators, *Sens. Actuators A*, 2010, **158**, p 149–160
8. M. Khol, *Shape Memory Microactuators*, Springer Book Series on Microtechnology and MEMS, 2004
9. M. Mertmann and G. Vergani, Design and Application of Shape Memory Actuators, *Eur. Phys. J. Spec. Top.*, 2008, **158**, p 221–230
10. P. Wollants, M. De Bonte, L. Delaye, and J.R. Roos, Thermodynamical Analysis of the Work Performance of a Martensitic Transformation Under Stressed Conditions, *Z. Metallk.*, 1979, **70**, p 146
11. E. Patoor, D.C. Lagoudas, P.B. Entchev, L.C. Brinson, and X. Gao, Shape Memory Alloys, Part I: General Properties and Modeling of Single Crystals, *Mech. Mater.*, 2006, **38**(5–6), p 391–429
12. D.C. Lagoudas, P.B. Entchev, P. Popov, E. Patoor, L.C. Brinson, and X. Gao, Shape Memory Alloys, Part II: Modeling of Polycrystals, *Mech. Mater.*, 2006, **38**(5–6), p 430–462
13. A. Bhattacharyya, L. Sweeney, and M.G. Faulkner, Experimental Characterization of Free Convection During Thermal Phase Transformations in Shape Memory Alloy Wires, *Smart Mater. Struct.*, 2002, **11**, p 411–422
14. M.A. Iadicola and J.A. Shaw, Rate and Thermal Sensitivities of Unstable Transformation Behavior in a Shape Memory Alloy, *Int. J. Plast.*, 2004, **20**, p 577–605
15. H. Meier and L. Oelschlaeger, Numerical Thermomechanical Modeling of Shape Memory Alloy Wires, *Mater. Sci. Eng. A*, 2004, **378**, p 484–489
16. B.-C. Chang, J.A. Shaw, and M.A. Iadicola, Thermodynamics of Shape Memory Alloy Wire: Modeling, Experiments, and Application, *Continuum Mech. Thermodyn.*, 2006, **18**, p 83–118
17. H. Soul, A. Yawny, F.C. Lovey, and V. Torra, Thermal Effects in a Mechanical Model for Pseudoelastic Behavior of NiTi Wires, *Mater. Res.*, 2007, **10**(4), p 387–394
18. P. Schlosser, D. Favier, H. Louche, and L. Orgéas, Experimental Characterization of NiTi SMAs Thermomechanical Behaviour Using Temperature and Strain Full-Field Measurements, *Adv. Sci. Technol.*, 2008, **59**, p 140–149
19. J.F. Smith et al., The Heat Capacity of Solid Ni-Ti Alloys in the Temperature Range 120 to 800 K, *J. Phase Equilib.*, 1993, **14**(4), p 494–500
20. C.O. Popiel, J. Wojtkowiak, and K. Bober, Laminar Free Convective Heat Transfer From Isothermal Vertical Slender Cylinder, *Exp. Therm. Fluid Sci.*, 2007, **32**, p 607–661
21. K.A. Bucker and J. Majdalani, Effective Thermal Conductivity of Common Geometry Shapes, *Int. J. Heat Mass Transf.*, 2005, **48**(8), p 4779–4796
22. C. Zanotti, P. Giuliani, A. Tuissi, S. Arnaboldi, and R. Casati, Response of NiTi SMA Wire Electrically Heated, *ESOMAT 2009 - The 8th European Symposium on Martensitic Transformations*, [N. 06037], P. Šittner, L. Heller, and V. Paidar, Eds., EDP Sciences, 2009, [www.esomat.org](http://www.esomat.org), doi:10.1051/esomat/200906037
23. M.G. Faulkner, J.J. Amalraj, and A. Bhattacharya, Experimental Determination of Thermal and Electrical Properties of Ni-Ti Shape Memory Wires, *Smart Mater. Struct.*, 2000, **9**, p 632–639
24. V. Novak, P. Šittner, G.N. Dayananda, F.M. Braz-Fernandes, and K.K. Maheshc, Electric Resistance Variation of NiTi Shape Memory Alloy Wires in Thermomechanical Tests: Experiments and Simulation, *Mater. Sci. Eng. A*, 2008, **481–482**, p 127–133
25. A. Sala, *Radiant Properties of Materials, Vol 21 of Physical Sciences Data*, Elsevier, New York, 1986